Acta Cryst B
STRUCTURAL SCIENCE
CRYSTAL ENGINEERING
MATERIALS

ISSN 2052-5206

Synthesis, chiral crystal structure, and magnetic properties of $Ba_3Ga_2O_5Cl_2$

Jeremy Rine,[a] Yongqi Yang,[b] Zhixue Shu,[a] Jianda Zhao,[a] Weiwei Xie[b] and Tai Kong[a,c]*

[a]Department of Physics, University of Arizona, Tucson, AZ 85721, USA, [b]Department of Chemistry and Chemical Biology, Rutgers University, Piscataway, NJ 08854, USA, and [c]Department of Chemistry and Biochemistry, University of Arizona, Tucson, AZ 85721, USA. *Correspondence e-mail: tkong@arizona.edu

Received 8 March 2022
Accepted 3 May 2022

Edited by T. B. Bekker, Siberian Branch of Russian Academy of Science, Russian Federation

Keywords: crystal structure; PXRD; barium; gallium; solid-state synthesis; magnetization; oxychloride.

CCDC reference: 2170191

Supporting information: this article has supporting information at journals.iucr.org/b

A new compound, $Ba_3Ga_2O_5Cl_2$, isostructural with $Ba_3Fe_2O_5Cl_2$, was synthesized by solid-state reaction in air. Through single-crystal and powder X-ray diffraction analysis, the crystal structure was determined to be cubic with chiral space group $I2_13$ and unit-cell parameter a = 9.928 (1) Å. The Ga^{3+} ions in $Ba_3Ga_2O_5Cl_2$ are coordinated by O atoms and form GaO_4 tetrahedra. Ten neighboring GaO_4 tetrahedra are further bridged through corner sharing and rotation along the body diagonal, producing the chiral structure. Magnetization measurements indicate temperature-independent diamagnetic behavior, which is qualitatively consistent with core diamagnetism from all the constituent elements.

1. Introduction

Alkaline earth metal oxychlorides host a wide variety of chemical structures showing emergent physical properties, such as superconductivity (Adachi *et al.*, 1998) and long-range magnetic ordering (Knee *et al.*, 2004). Among these systems, compounds with the general chemical formula $AE_3M_2O_5Cl_2$ (AE = Ca, Sr or Ba; M = trivalent metal) can take two distinct crystal structures despite the similarity in composition. $Sr_3Fe_2O_5Cl_2$, for example, forms a layered perovskite-like structure with the space group $I4/mmm$ (Ackerman, 1991). This layered structure is similar to the Ruddlesden–Popper (RP) phase found in cuprate superconductors (Adachi *et al.*, 1998), where Cl atoms replace apical O atoms in a regular octahedron in the RP phase. The metal–oxygen planar network can produce long-range antiferromagnetic ordering (Knee *et al.*, 2004). Instead of retaining the perovskite-like structure, replacement of the alkaline earth or metal site can also yield a cubic phase, examples being $Ba_3Fe_2O_5Cl_2$ (Leib & Müller-Buschbaum, 1985) and $Sr_3Ga_2O_5Cl_2$ (Leib & Müller-Buschbaum, 1988). $Ba_3Fe_2O_5Cl_2$ was reported to order antiferromagnetically at 564 K, with field-induced electric polarization (Abe *et al.*, 2020). Recently, cubic $Sr_3Ga_2O_5Cl_2$ has been used as the host compound to design light-emitting diodes (LEDs) with Bi or Eu doping (Ci *et al.*, 2015; Lee *et al.*, 2010; Su *et al.*, 2010). It is unclear which factors determine the final selection of the crystal structure in this family of compounds. As part of an exploration of new compounds with this composition, we report the discovery of a new cubic phase, $Ba_3Ga_2O_5Cl_2$, which may offer greater tunability in the optical spectrum in LED light.

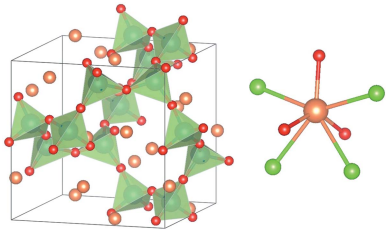

Table 1
The crystal structure and refinement for $Ba_3Ga_2O_5Cl_2$ at 300 K.

Chemical formula	$Ba_3Ga_2O_5Cl_2$
Formula weight (g mol^{-1})	702.36
Space group	$I2_13$
Unit-cell dimensions (Å)	a = 9.928 (1)
Volume (Å^3)	978.6 (5)
Density (calculated) (Mg m^{-3})	4.767
Absorption coefficient (mm^{-1})	17.849
F(000)	1216
2θ range (°)	5.80–69.56
Total reflections	759
Independent reflections	559 (R_{int} = 0.0152)
Refinement method	Full-matrix least-squares on F^2
Data, restraints, parameters	559, 0, 21
Flack factor	0.005 (0.043)
Final R indices	R_1 [$I > 2\sigma(I)$] = 0.0216; wR_2 [$I > 2\sigma(I)$] = 0.0464
	R_1 (all) = 0.0258; wR_2 (all) = 0.0722
Weighting scheme	$w = 1/[\sigma^2(F_o^2) + 19.8694P]$; $P = (F_o^2 + 2F_c^2)/3$
Largest difference peak and hole (e Å^{-3})	1.897, −1.551
R.m.s. deviation from mean (e Å^{-3})	0.438
Goodness-of-fit on F^2	1.325

Computer programs: *APEX2* (Bruker, 2009), *SAINT* (Bruker, 2009), *SHELXT2018* (Sheldrick, 2015*a*), and *SHELXL2018* (Sheldrick, 2015*b*).

2. Experimental methods

Polycrystalline $Ba_3Ga_2O_5Cl_2$ was prepared *via* solid-state reaction. The starting materials, $BaCO_3$ (Alfa Aesar, 99.8%), $BaCl_2{\cdot}2H_2O$ (Alfa Aesar 99+%), and Ga_2O_3 (Alfa Aesar 99.99%), were mixed in a 2:1:1 molar ratio and ground together in an agate mortar. The ground powder was heated to 850 °C in an alumina crucible in air. Several intermediate regrindings were performed to improve the purity of the target phase. Small single crystalline $Ba_3Ga_2O_5Cl_2$ was obtained by adding a 10% excess of $BaCl_2$ as solvent to the starting material, under the same synthesis conditions. $Ba_3Ga_2O_5Cl_2$ powder has an off-white color and is weakly reactive towards air over an exposure time of months.

The crystal structure of $Ba_3Ga_2O_5Cl_2$ was first determined by single-crystal X-ray diffraction (SC-XRD). The structure was solved and refined using the *SHELX* software package (Sheldrick, 2015*a*,*b*). The integration of the data using a cubic unit cell yielded a total of 759 reflections to a maximum 2θ angle of 69.56° (0.62 Å resolution), of which 559 were independent (R_{int} = 0.0152 and R_{sig} = 0.0338) and 543 (97.14%) were greater than 2$\sigma(F^2)$. The final unit-cell parameters of a = 9.9282 (16) Å and V = 978.6 (5) Å^3 are based upon the refinement of the *XYZ*-centroids of 637 reflections above 20$\sigma(I)$ with 8.237 < 2θ < 69.83°. Data were corrected for absorption effects using the multi-scan method (*SADABS*; Bruker, 2009). The ratio of minimum-to-maximum apparent transmission was 0.815. The final anisotropic full-matrix least-squares refinement on F^2 with 21 variables converged at R_1 = 0.0216 for the observed data and at wR_2 = 0.0722 for all data.

For crystal structure refinement, a cube-shaped transparent single crystal of $Ba_3Ga_2O_5Cl_2$ was chosen, mounted on the Kapton sample holder and measured using a Bruker Eco Quest single-crystal X-ray diffractometer with Mo $K\alpha$ radiation (λ = 0.71076 Å) at 300 K. Each reflection frame was exposed for 10 s and integrated with the *SAINT* software package (Bruker, 2009) using a narrow-frame algorithm. Powder X-ray diffraction (PXRD) analysis was carried out using a Bruker Discover X-ray diffractometer (Cu $K\alpha$ radiation) equipped with a microfocus source. Le Bail refinements were performed using *GSAS* software (Larson & Von Dreele, 2000; Toby, 2001). The crystal structure was plotted using *VESTA* (Momma & Izumi, 2011).

Table 2
Atomic coordinates and equivalent isotropic atomic displacement parameters (Å^2) for $Ba_3Ga_2O_5Cl_2$.

U_{eq} is defined as one third of the trace of the orthogonalized U_{ij} tensor.

	Wyckoff	x	y	z	Occ.	U_{eq}
Ba	12*b*	0.3416 (1)	0	$\frac{1}{4}$	1	0.0118 (2)
Ga	8*a*	0.3454 (1)	0.3454 (1)	0.3454 (1)	1	0.0065 (3)
Cl	8*a*	0.0587 (2)	0.0587 (2)	0.0587 (2)	1	0.0188 (8)
O1	8*a*	0.2401 (5)	0.2401 (5)	0.2401 (5)	1	0.0083 (16)
O2	12*b*	0.6077 (10)	0	$\frac{1}{4}$	1	0.0142 (16)

On the basis of the final model, the calculated density was 4.767 Mg m^{-3} and the value of F(000) was 1216 e$^-$. Detailed refinement results and atomic positions are available in Tables 1 and 2. PXRD data were also used to confirm the bulk phase purity of each batch of produced materials.

Temperature-dependent (1.8–300 K) magnetization measurements were conducted using a Quantum Design (QD) PPMS Dynacool measurement system with a vibrating sample magnetometer. Powder samples were loaded into a QD plastic capsule for each measurement.

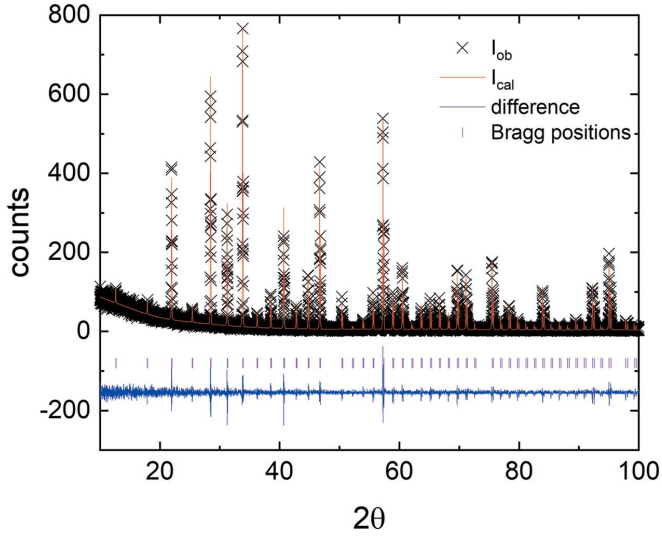

Figure 1
Powder X-ray diffraction (PXRD) data for $Ba_3Ga_2O_5Cl_2$. Experimental data are shown as black crosses, calculated intensity as a solid red line, difference as a solid blue line and expected Bragg positions as magenta ticks.

3. Results and discussion

Fig. 1 shows the powder diffraction data, with Le Bail fitting shown in red. In general, all the diffraction peaks can be indexed with the crystal structure refined through SC-XRD. A small χ^2 value of 1.46 indicates a good purity of the synthesized powder. A platinum crucible was also used to synthesize $Ba_3Ga_2O_5Cl_2$, but showed no detectable difference in the sample color or the powder diffraction results.

The refined crystal structure of $Ba_3Ga_2O_5Cl_2$ is shown in Fig. 2 and is similar to that of $Ba_3Fe_2Cl_2O_5$ (Leib & Müller-Buschbaum, 1985) and $Sr_3Ga_2O_5Cl_2$ (Leib & Müller-Buschbaum, 1988) but not $Sr_3Fe_2O_5Cl_2$. There are five different atomic sites in a unit cell. Except for O atoms, which occupy two different atomic sites, divalent Ba, trivalent Ga, and Cl atoms each occupy a unique site. In contrast to the perovskite-like two-dimensional Fe–O layers in $Sr_3Fe_2O_5Cl_2$ with an octahedral coordination, the Ga–O tetrahedra form a three-dimensional network in $Ba_3Ga_2O_5Cl_2$. Each Ga–O tetrahedron is slightly distorted, with two Ga—O bond lengths of 1.863 (2) and 1.811 (10) Å. The Ba atoms are coordinated by four Cl and three O atoms in a heavily distorted decagon [Fig. 2(*b*)]. The Ba—O bond lengths are 2.642 (10) or 2.590 (3) Å and the Ba—Cl bond lengths are 3.2730 (19) or 3.440 (3) Å. Fig. 2 shows the Ga—O tetrahedron, with Ba atoms filling the empty spaces. Cl atoms are solely bonded to Ba^{2+} cations, which have been omitted for simplicity. Corner-sharing Ga–O tetrahedra form a three-dimensional network, which can be viewed as distorted rings that each contain ten Ga–O tetrahedra. Neighboring Ga–O tetrahedra are linked *via* corner-sharing O atoms that are both bent and rotated with respect to each other to form a Ga—O—Ga angle of 151.1 (6)°. The overall noncentrosymmetric structure may be useful for optical second harmonic generation.

As discussed above, the family of compounds with the chemical formula $AE_3M_2O_5Cl_2$ (AE = Ca, Sr or Ba; M = trivalent metal) primarily takes on two different types of structure: a layered perovskite-type (Ackerman, 1991) or a cubic type with corner-sharing tetrahedra (Leib & Müller-Buschbaum, 1985). Compared to other perovskites that show

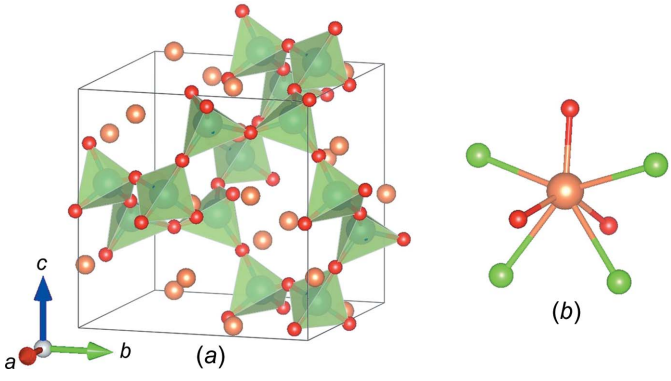

Figure 2
(*a*) The unit cell of $Ba_3Ga_2O_5Cl_2$, showing only the Ba–O polyhedral network and Ba atoms. (*b*) The local coordination of Ba atoms. O atoms are represented by red, Cl atoms by green, Ba atoms by brown and Ga atoms by blue spheres.

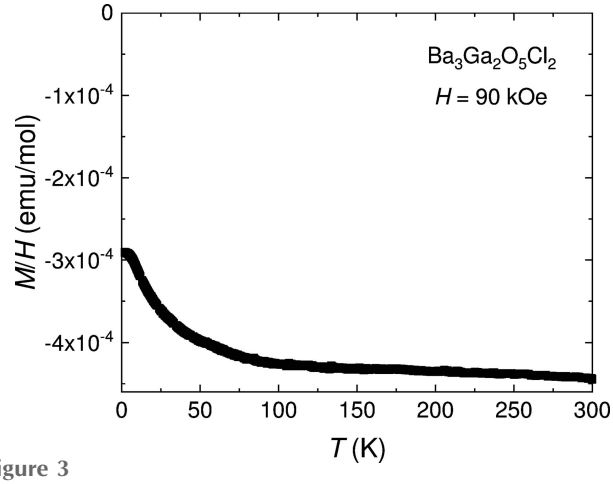

Figure 3
Temperature-dependent magnetization data of $Ba_3Ga_2O_5Cl_2$ measured at 90 kOe in the temperature range from 300 to 1.8 K.

structural variation according to the alkali earth elemental radii, and thus the Goldschmidt tolerance factor (Goldschmidt, 1926), the structural stability for $AE_3M_2O_5Cl_2$ appears to be also dependent on the coordination preference of the transition-metal site. This is illustrated, for example, in $Sr_3Fe_2O_5Cl_2$, with approximately 40% of tetrahedra favoring aluminium substitution (Dudev *et al.*, 2006) on the Fe site which turns the structure from layered into cubic (Leib & Müller-Buschbaum, 1988). Gallium tends to occupy the center of a tetrahedron (Dudev *et al.*, 2006) and is thus found to form a cubic structure in $Sr_3Ga_2O_5Cl_2$ (Leib & Müller-Buschbaum, 1988). With barium ions being 14% larger than strontium ions (Shannon, 1976), the cubic structure is retained in $Ba_3Ga_2O_5Cl_2$ in this study. Increasing the difference in the ionic size between the AE and M site atoms could still stabilize the cubic structure, such as in the case of $Ba_3Fe_2O_5Cl_2$. Therefore, for large barium compounds, larger M-site atoms, such as rare earths, could help stabilize the layered structure (Besara *et al.*, 2018; Su *et al.*, 2018). The trivalent indium ion, with a slightly greater tendency to form a tetrahedron over an octahedron (Dudev *et al.*, 2006), retains the layered structure, likely due to the ionic size preference (Shannon, 1976). It is as yet unclear if the $AE_3M_2O_5Cl_2$ structures favor particular d-orbital filling in addition to the ionic size and coordination requirements. So far, most of the reported compounds have either filled or close to half-filled d-orbitals.

The temperature-dependent magnetization of $Ba_3Ga_2O_5Cl_2$ is shown in Fig. 3. It shows a near temperature-independent diamagnetic response from room temperature to 1.8 K. A slight upturn below 100 K is likely due to the presence of a small amount of paramagnetic impurity. The diamagnetic susceptibility of around -4×10^{-4} emu mol^{-1} is qualitatively in agreement with the combination of core diamagnetism from all the elements in the compound (Bain & Berry, 2008). Temperature-dependent resistance measurements to determine the electrical band gap were not successful due to the large resistance value of the sample. Preliminary reflectivity measurements did not show a clear signature of optical absorption above 300 nm.

4. Summary

We report the synthesis, crystal structure, and magnetic properties of a new barium gallium oxychloride. Off-white $Ba_3Ga_2O_5Cl_2$ can be synthesized in air *via* solid-state reaction. It crystallizes in a cubic noncentrosymmetric structure, similar to $Ba_3Fe_2O_5Cl_2$, with the space group $I2_13$ and unit-cell parameter a = 9.928 (1) Å. The magnetization of $Ba_3Ga_2O_5Cl_2$ is primarily contributed to by the core diamagnetism of each element. A more detailed optical investigation would be of interest to reveal the optical band gap, as well as the potential design of LEDs.

Acknowledgements

We would like to thank Srin Manne, Shu Guo, and Paul Lee for their help in this project. This work is supported by University of Arizona startup funds and an NSF grant. The work at Rutgers is supported by an NSF grant.

Funding information

Funding for this research was provided by: National Science Foundation, Directorate for Mathematical and Physical Sciences (grant No. 1757878); National Science Foundation, Directorate for Mathematical and Physical Sciences (grant No. 2053287).

References

Abe, N., Shiozawa, S., Matsuura, K., Sagayama, H., Nakao, A., Ohhara, T., Tokunaga, Y. & Arima, T. (2020). *Phys. Rev. B*, **101**, 180407.

Ackerman, J. F. (1991). *J. Solid State Chem.* **92**, 496–513.

Adachi, S., Tatsuki, T., Tamura, T. & Tanabe, K. (1998). *Chem. Mater.* **10**, 2860–2869.

Bain, G. A. & Berry, J. F. (2008). *J. Chem. Educ.* **85**, 532.

Besara, T., Ramirez, D. C., Sun, J., Falb, N. W., Lan, W., Neu, J. N., Whalen, J. B., Singh, D. J. & Siegrist, T. (2018). *Inorg. Chem.* **57**, 1727–1734.

Bruker (2009). *APEX2, SAINT*, and *SADABS*. Bruker AXS Inc., Madison, Wisconsin, USA.

Ci, Z., Guan, R., Nie, K., Liu, L., Han, L., Zhang, J. & Wang, Y. (2015). *Mater. Res. Bull.* **70**, 822–826.

Dudev, M., Wang, J., Dudev, T. & Lim, C. (2006). *J. Phys. Chem. B*, **110**, 1889–1895.

Goldschmidt, V. M. (1926). *Naturwissenschaften*, **14**, 477–485.

Knee, C. S., Field, M. A. L. & Weller, M. T. (2004). *Solid State Sci.* **6**, 443–450.

Larson, A. C. & Von Dreele, R. B. (2000). General Structure Analysis System (*GSAS*). Report LAUR 86-748. Los Alamos National Laboratory, New Mexico, USA.

Lee, J., Choi, J., Zhang, X., Lee, J. B., Park, K. & Kim, J. (2010). *Mater. Lett.* **64**, 768–770.

Leib, W. & Müller-Buschbaum, H. (1985). *Z. Anorg. Allg. Chem.* **521**, 51–56.

Leib, W. & Müller-Buschbaum, H. (1988). *Monatsh. Chem.* **119**, 157–164.

Momma, K. & Izumi, F. (2011). *J. Appl. Cryst.* **44**, 1272–1276.

Shannon, R. D. (1976). *Acta Cryst.* A**32**, 751–767.

Sheldrick, G. M. (2015*a*). *Acta Cryst.* A**71**, 3–8.

Sheldrick, G. M. (2015*b*). *Acta Cryst.* C**71**, 3–8.

Su, J., Bum Lee, J., Won Park, K., Park, J., Su Kim, J., Kung, P. & Kim, S. M. (2010). *Proc. SPIE*, **7617**, 76171M.

Su, Y., Tsujimoto, Y., Fujii, K., Tatsuta, M., Oka, K., Yashima, M., Ogino, H. & Yamaura, K. (2018). *Inorg. Chem.* **57**, 5615–5623.

Toby, B. H. (2001). *J. Appl. Cryst.* **34**, 210–213.